Estuarine, Coastal and Shelf Science 252 (2021) 107246

Contents lists available at ScienceDirect

Estuarine, Coastal and Shelf Science

journal homepage: http://www.elsevier.com/locate/ecss

Saline intrusion in the Ganges-Brahmaputra-Meghna megadelta

Lucy M. Bricheno *, Judith Wolf, Yujuan Sun

National Oceanography Centre, Liverpool, UK

ARTICLE INFO

Keywords:
Delta
Salt intrusion
Bangladesh
Numerical modelling
Climate change
Tides

ABSTRACT

In the fertile Ganges-Brahmaputra-Meghna (GBM) delta, which spans the boundary from West Bengal in India and Bangladesh, the availability of freshwater is crucial to subsistence livelihoods and protected ecosystems. Controlled by large tides and widely variable river discharge, the delta experiences rising river salinity and salt intrusion, as well as seasonal flooding during the monsoon.

Future climate change is projected to increase rainfall in South Asia and river discharge in the GBM system. We address how this process might combine with sea-level rise (SLR) to control future river salinity. Model experiments designed using a range of SLR and climate change scenarios are performed to investigate the forces controlling river salinity in the delta. A flexible mesh modelling approach allows us to investigate the impacts at a wide range of time and space scales.

In future projections the disparity between wet and dry season salt intrusion intensifies. In the future, SLR acts to increase river salinity in the GBM delta. During the dry season, this effect is worsened by reduced river discharge. In the wet season, this can be mitigated in the eastern part of the delta by larger seasonal river flows. The central and western delta is dominated by SLR, leading to increased salt intrusion all year round, impacting on water resources and agricultural productivity. In the context of an intensifying hydrological cycle, these conclusions have implications for similar tide-dominated deltas, where SLR can increase tidal range, and therefore exacerbate salt intrusion.

1. Introduction

River deltas form, usually, where a sediment-laden river meets the sea, depositing sediment, which builds up into a triangular-shaped piece of land, named for the Greek letter Δ. Globally, river deltas are very important for human occupation, providing low-lying fertile land, which can provide subsistence for some of the poorest people on the planet, as well as being the location of many mega-cities (Syvitski et al., 2009). Deltas can be classified as wave-, tide- or river-dominated (Galloway, 1975), although Caldwell et al. (2019) point out that the river and sediment load are the delta-building processes, whereas waves and tides are generally destructive (Nienhuis et al. 2015, 2018). At the same time, they are exposed to natural processes of erosion and flooding, especially for tropical deltas exposed to the risks of tropical storms, and at the mercy of fluctuations in seasonal rainfall, such as the annual monsoon in South Asia. Deltas are also being increasingly threatened by sea level rise (SLR), due to external factors like global warming, as well as local subsidence (Syvitski et al., 2009). Although the majority of deltas appear to be gaining land to date (Nienhuis et al., 2020), as SLR accelerates (Nerem et al., 2018) this may change in the future. They are also an interface between the high-salinity water of the sea and the freshwater from the river and the water quality of the brackish water in the delta distributaries can have important implications for human health and agriculture. Sea-level rise, combined with fluctuating river discharge is causing an increase in salinity intrusion in many deltas worldwide (White and Kaplan, 2017), e.g. Mekong (Eslami et al., 2019); Yangtze (Dai et al., 2011); Ganges-Brahmaputra-Meghna (GBM) (Sherin et al., 2020); Pearl River (Hong et al., 2020; Liu et al., 2018).

This paper identifies the key factors controlling salinity intrusion in the low elevation coastal zone (LECZ), and investigates how future changes in climate, precipitation, discharge, and SLR affect river salinity. Climate change is predicted to accelerate the water cycle (Kundzewicz, 2008), which can an lead to benefits through increases in annual runoff, the advantages will be weighed with increased variability and seasonal runoff shifts exacerbating salt intrusion. Changing river discharge and SLR will also impact the tidal dynamics: an analysis of changing tides and currents in the wet and dry periods is performed, to understand better how these mechanisms will influence seasonal

* Corresponding author.
E-mail address: luic@noc.ac.uk (L.M. Bricheno).

https://doi.org/10.1016/j.ecss.2021.107246
Received 28 August 2020; Received in revised form 21 January 2021; Accepted 28 January 2021
Available online 25 February 2021

salinity. We investigate the tidal and seasonal controls on salinity, and also address the interaction of coastal and river salinity, which will in turn impact upon the water table, drinking water from tube wells and soil salinity. Lastly we draw conclusions about how these climate driven changes may impact freshwater availably during rice growing seasons. Though this work is specific to Bangladesh, we believe the conclusions to be applicable to similar deltaic environments where the tide dominates.

2. Site description

The GBM delta is highly fertile, being intensively farmed with rice as a primary crop; to maximise production, river water is used for irrigation, and therefore water quality and local salinity are important to agriculture. Water salinity below 1 is the threshold for drinking water, while the critical salinity level for agriculture is 2 (Dasgupta et al., 2014). In recent years there has been an increase in river salinity (Dasgupta et al., 2014). Clarke et al. (2015) state that once the dry season irrigation water exceeds a salinity of 5, the monsoon rainfall is no longer able to leach out the dry season salt deposits, leading to further salt accumulation. Soil salinity has also been increasing in coastal Bangladesh over the last 30 years (Salehin et al., 2018). Soil salinity has a complicated spatial pattern, determined in part by river salinity, groundwater salinity, and management practices (Salehin et al., 2018). In unprotected areas, brackish water can inundate large areas of land, driven by natural changes in water levels through tidal and seasonal processes. Agricultural land is often separated from the rivers by polders/embankments, to prevent seawater overtopping. Conversely, saline aquaculture ponds can be dug, for cultivation of brackish, or brine shrimp. In areas protected by polders, inundation can still occur through embankment breaches, and seepage (Huq and Shoaib, 2013). Breaches of sea-defences can also occur as a result of extreme events, such as storm surges generated by cyclones. Therefore, river salinity is an important factor throughout the delta (Bricheno and Wolf 2018).

With an average freshwater discharge of around 40,000 m^3s^{-1} (Whitehead et al., 2015a), and peak flows of 138,700 m^3s^{-1} during floods, the GBM river system has the third largest discharge worldwide (FAO, 2016). The GBM river delta is a low-lying fertile area covering over 100,000 km^2 in India (West Bengal) and Bangladesh, and is thus classified as a megadelta (Milliman and Meade 1983; Brown and Nicholls 2015). Bangladesh experiences a subtropical monsoon climate: a dry season (October–March), a hot summer (March–June), and a wet season (June–October) (FAO, 2016). High river discharge in the annual monsoon rainy season acts to flush-out saltwater, and feeds the offshore freshwater plume in the northern Bay of Bengal (Howden and Murtugudde, 2001). During the wet season, some flushing of the Western Estuarine section (WES) can also occur, counteracting the salt intrusion (e.g. Shaha and Cho (2016)) Through the Holocene the active channel of river GBM system has moved from west to east (Allison, 1998). In the present day the active river mouth is constrained to the east by the Chittagong hill tract, and the majority of the freshwater is channelled through the Padma river (Brammer, 2014). Around 10% of the total volume of the Ganges discharges through the Gorai river channel Bain et al. (2019), and on the Bangladesh side this is the only source of freshwater to the WES. As the GBM is tide dominated, there are some inactive (unconnected) river channels behaving as tidal creeks (in the WES particularly), but these are not considered as individual sources of freshwater. Across the border with India, the Hooghly river also brings freshwater to the WES and Sundarbans, with peak flows exceeding 10, 000 m^3s^{-1} (Biswas et al., 2007).

River management within and outside of Bangladesh can have far-reaching impacts on the whole GBM catchment. Higgins et al. (2018) details India's National River Linking Project (NRLP), and derive potential changes in discharge (reduction of 6% annual water flow) and sediment delivery to the delta. For example, the environmental impacts of the Farraka Dam on Hooghly have been discussed by Sinha (2004). Whitehead et al. (2015b) state that 'should large scale water transfers upstream of Bangladesh be constructed, these have the potential to reduce flows and divert water away from the delta region depending on the volume and timing of the transfers. This could have significant implications for the delta in terms of saline intrusion, water supply, agriculture and maintaining crucial ecosystems such as the mangrove forests, with serious implications for people's livelihoods in the area.' Higgins et al. (2018) also predict that 'Climate-related salinity incursion in rivers and deltas will be exacerbated by the decrease in river mouth discharge brought about by the NRLP. The discharge from the Gorai is decreasing, and has halved in the past 50 years, due to a combination of anthropogenic controls such as land-use change, water diversion, and river management (Bain et al., 2019).

The GBM river system also delivers a high suspended sediment load of around 1×10^9 tonnes of suspended sediment (Islam et al., 2001). The northern Bay of Bengal is mesotidal, with tidal ranges at the coast varying from 2 m to over 4 m in places (Murty and Henry, 1983). Large tides at the coast can penetrate far inland, with tidal variability being observed as far as 200 km inland (Bricheno et al., 2016). The semi-diurnal tide generates strong mixing, and carries seawater inland. This competes with a seasonal movement of the freshwater front, as large river discharge brings a strong stratifying effect. During the dry season high salinity sea water penetrates further inland (CSIRO et al., 2014), and this salinity intrusion is enhanced by rising sea levels (Dasgupta et al., 2014).

The GBM delta is a tide-dominated delta in common with the Amazon, Irrawaddy, Indus, Tigris, Yangzte, and Mekong. It also experiences one of the largest river discharges in common with the Amazon, Congo, Orinoco, Yangtze, Mekong, and Irrawaddy. Salt intrusion is identified as a serious problem in many estuaries under the impact of global climate change and local anthropogenic activities. Zhang et al. (2010) investigated the river discharge-salt intrusion relation in the Pearl River estuary, noting that the salt intrusion length is dependent on the river discharge. Hoitink and Jay (2016) summarized the estuary and tidal river properties for the Amazon, Columbia, Saint Lawrence, and the Yangtze rivers, showing no salinity intrusion at all in the Amazon (Gallo and Vinzon, 2005), while estimates of the salt intrusion length in the Saint Lawrence estuary could reach 500 km Matte et al. (2014). The tides in the GBM delta are large, and can propagate long distances into the delta. These tides generate strong mixing, bringing salt water inland and controlling the position of the river plume. On the other hand, the presence of freshwater is known to modify the tides significantly (see e. g. Horrevoets et al. (2004); Sassi and Hoitink (2013); Leonardi et al. (2015); Cao et al. (2020). The GBM delta is macro-tidal, with the largest tidal range seen in the northeast and northwest 'corners' of the Bay of Bengal. However, due to the asymmetry of the freshwater plume, the impact of the tides on salt transport changes across the delta. In the east along the largest channel of the GBM, the freshwater plume can shield against salt intrusion. However, in the WES where discharge is low, the inland extension of the large tides is able to penetrate a lot further inland.

The GBM is the site of the Sundarbans mangrove forest, inscribed as a UNESCO World Heritage Site since 1997. This is the world's largest mangrove forest whose ecosystem depends on a narrow range of salinity conditions. The other region where river and soil salinity is critical is in the central estuarine section (CES), where some of the poorest communities are living in marginal environments at the edge of useable irrigation waters (Johnson et al., 2016b; Johnson and Hutton, 2018). Changes in river and soil salinity have potential consequences for land use practices and livelihoods for the delta population. The coastal area constitutes 30% of cultivable lands in Bangladesh of which about 53% are affected by high salinities (Haque 2006). For example, some farmers have already chosen to convert freshwater rice paddies to salt water shrimp farms, which could take decades to reverse if required (Johnson et al., 2016a). Understanding how changing climate may affect future salinity levels is therefore an important research topic, particularly

changes in the monsoon rains, leading to changing freshwater flow. Khanom and Salehin (2012) state that saline intrusion is very important during March–May (the dry season). This affects crop yield and drinking water. There are different associated risks when considering the possible sources of both drinking and irrigation waters. In terms of water quality, arsenic is major problem in Bangladesh, but has been well studied (e.g. Chowdhury et al. (2000) Sohel et al. (2009)). In order to counter the arsenic problems, the National Policy for Arsenic Mitigation (NPAM) encouraged a return to the use of surface or very shallow groundwater (Ahmed et al., 2006). However, surface water has an increased risk from microbial pathogens in waste and sewage. Drinking water is often extracted from groundwater and shallow tube-wells, even though the salinity of these waters can often exceed safe drinking water thresholds (Khanom and Salehin, 2012). In Bangladesh and West Bengal, high salinities in drinking water (salinity above 1) cause health problems such as diarrhoea and high blood pressure (hypertension) see e.g. Alcamo et al. (2003), Ahmed et al. (2018). Khan et al. (2011) state that "the problem of saline intrusion into drinking water is likely to be exacerbated by climate change-induced sea-level rise."

Clarke et al. (2015) state that both climate variability and saline intrusion are important drivers of determining the productivity of dry season agriculture in coastal Bangladesh by the end of 21st century. It is particularly important to get the dry season modelled correctly, to identify when farmers can irrigate and have 3 crops per year (Huq and Shoaib, 2013). Payo et al. (2017) combine river and groundwater salinity to calculate the soil moisture deficit, stating that to do so you "need a good representation of ground water depth and ground water salinity and water and salt fluxes from river and coastal flooding". The river delta is a complex region of interconnected river channels, and the interactions between river and tide must be correctly represented in order to capture the salinity distribution in this area. Observations of river and soil salinity are very scarce in this region, thus a numerical modelling approach is needed to give detailed spatial and temporal predictions.

Sea level rise is an important consideration for the future of all deltaic environments, including the Bangladesh coast. Much work has been done exploring the causes and rates of sea-level rise in Bangladesh e.g. Han et al. (2010) Brown and Nicholls (2015) Pethick and Orford (2013), CEGIS (2006). Low-lying deltas are sensitive to both eustatic change (from alteration in the volume of water in the ocean), and also relative changes, through tectonic subsidence, sediment compaction and groundwater extraction (e.g. Pethick and Orford (2013)). Reduced river discharge and therefore slower flow speeds, can lead to more sediment deposition, and channel infilling, while the erection and maintenance of polders cuts-off sediment supply and contribute to changes in lower land levels locally (Wilson et al., 2017). Local changes in morphology and river geometry can also have impacts on tidal behaviour (see appendix). Future projections have also been made to gauge the possible future sea-level change and impacts both globally and regionally e.g. Vousdoukas et al. (2018), Jevrejeva et al. (2016), Jackson and Jevrejeva (2016), Nicholls and Mimura (1998). In this manuscript we will not investigate the causes of changing sea-level, but rather focus on the response of the delta's hydrodynamics to these predicted external changes.

3. Methods

When modelling the GBM delta we must accurately simulate both ocean and inland river conditions simultaneously. The FVCOM model has been used at the interface of land and sea in a variety of river, coast, and estuarine environments, for example the Pearl River (Yuan and Zhu, 2015), Chesapeake Bay (Tian 2019) the Delaware River (Zhang and Wei, 2007), and Darwin Harbour (Li et al., 2012). We believe this to be a good compromise between a 1-D inland river flow model and a 3-D deep ocean model. This paper presents results from a flexible-grid model which has been used to simulate tides and river salinity in the GBM delta (Bricheno et al., 2016). FVCOM is an unstructured finite volume, 3D baroclinic model which was developed for use in estuarine systems and has since been applied to wider areas (Chen et al., 2003). FVCOM has the ability to include river discharge and flooding/drying inland, as well as representing the tides and baroclinic currents offshore as well as capacity to model sea-level rise.

Our configuration of FVCOM focusses on the processes within the delta, however the model must be informed by wider ocean and catchment models. For orientation, the extent of the models used is presented in Fig. 1. The left panel shows the extent of the catchment, ocean, and delta models, and the right panel names rivers and shows locations used for tidal analysis. Note that when referring to salinity it will be unitless, using the Practical Salinity Scale. The FVCOM model has been configured with 11 vertical levels and variable horizontal resolution between 10 km (at the open boundary) and 50 m, within narrow river channels. The challenge in constructing this model grid was to generate a good-quality mesh and bathymetry which allows the model to produce accurate flows through the delta region. Another limitation was lack of available data for model validation. Nonetheless, available observations of tidal water levels within the delta have been used to validate the basic hydrodynamics (Bricheno et al., 2016). FVCOM was able to accurately model the tidal ranges in the central delta, however there was some under-prediction of the tidal range in the Sundarbans forest region, and within the lower Meghna, where bathymetry is less accurate. The configuration presented here has been validated for historic water levels and tidal behaviour. This is the first time it has been assessed for skill in representing river salinity and baroclinic processes, before using the model to make future projections.

This model is here used to investigate river salinity within the delta, and how the distribution of salt and freshwater is controlled by a balance between tidal dynamics and hydraulic control. This is a unique approach, as we can combine future projections of mean SLR and offshore salinity, with projected changes in the hydrological cycle driving river discharge under future climate. At the open boundary the model is forced by hourly ocean tidal data and daily temperature and salinity from the Bay of Bengal GCOMS model (Kay et al., 2015).

Inland, the position of the coastline, and therefore hard limit on inundation is defined based on the results from Rahman et al. (2013) and Haque et al. (2016). Their Delft-3D model (which covers all land and sea points in the GBM delta) was run for an extreme flood condition, and this high-water extent was taken as the limit of river channels in the FVCOM domain. The model configuration then allows inundation and flooding up to this pre-defined high water mark, and thus can accommodate some encroachment due to future sea-level rise. Once this lateral extent of flooding has been exceeded, the river channels will only deepen in the vertical, which could lead to artificially large water depths, if the model channels are too narrowly constrained (Bricheno et al., 2016).

River discharge is applied as an upstream boundary condition: a volume of freshwater is introduced to the model at the northern boundary of the model (24° N, 89° E). The daily discharge volume rate comes from the hydrological INCA model (Wade et al., 2002), and the model configuration covering the whole of the GBM river systems used is described in Whitehead et al. (2015b). This catchment model is then driven by precipitation from a high-resolution (25 km) regional climate model over the south Asia region (Caesar et al., 2015; Caesar and Janes, 2018). The INCA model has been validated against historic river discharge, and then run forward for future time-slice projections under scenarios detailed in Table 1. Meteorological forcing is not applied locally in the delta model, but the surface freshwater flux input to INCA comes from the high resolution regional climate model projections of Caesar et al. (2015).

We have neglected a direct input of freshwater (through rainfall over the model extent). However, believe this to be a reasonable assumption (and avoids double counting), since this surface freshwater flux has been included in the catchment model, the river discharge used in our model already includes precipitation, evaporation over the whole delta region.

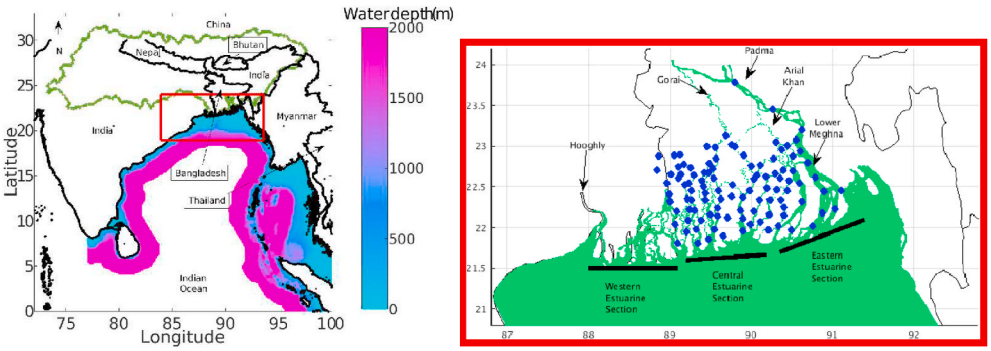

Fig. 1. Extent of model domains used (left). The catchment of the GBM is shown in green, coastline and national boundaries in black, and the FVCOM within the are inscribed in red. The coloured area shows the model bathymetry used in the ocean model GCOMS, whose domain follows a strip around the coast. The right hand panel shows locations used for analysis in section c, and labels some river and region names. (For interpretation of the references to colour in this figure legend, the reader is referred to the Web version of this article.)

Table 1
Summary of scenario runs presented, including scenarios used for atmospheric forcing. Details of the climate and management strategies can be found in Caesar et al. (2015).

Scenario	Description	Climate & management	MSLR (cm)	Year	Discharge (m^3)
Historic	Historic	Historic	0.0	1998–1999	9,054,014
1	Baseline	Q0 + Business as Usual	0.0	2000–2001	9,928,407
2	Mid century	Q0 + Business as Usual	31.96	2047–2048	13,979,424
3	Mid century	Q8 + Less Sustainable	27.06	2050–2051	10,011,085
4	End century	Q8 + Less Sustainable	58.77	2082–2083	16,517,208
5	End century	Q0 + Business as Usual	59.01	2097–2098	10,978,254

Nishat and Rahman (2009) find that about 92–93% of the surface water flowing through Bangladesh is generated in the upstream GBM in catchment areas that are outside the country. The Ganga river system drains an area of approximately 1,087,300 km^2, while the surface area of rivers in the FVCOM model is: 29,546 km^2, i.e. the river channel area in the FVCOM model accounts for around 2.5% of the total catchment of the INCA model, therefore we have decided to neglect the input of evaporation/precipitation directly into modelled river channels. The FVCOM model then acts as a series of river distributaries, connecting the river catchment model with the ocean conditions offshore. As we are interested in salt intrusion during the dry season, single year runs representing a 'snapshot' condition are run, beginning and ending on 1st July (thus initialising the model from high-flow conditions). For each scenario year the model is started from rest during a flood condition, and the freshwater is then allowed to flow through the distributaries, which ensures that the modelled river channels start in an active state, and the estuarine system is well connected.

3.1. Future scenario experiments

The aim of our experiments is to understand the impact of rising sea-levels and changing river discharge on future river salinity. To this end five scenarios were run: one as a baseline, and four futures (detailed in Table 1). The four futures were chosen to represent a mid-century period (2030–2059) and a late century period (2070–2099), with a range of flow conditions. To identify suitable candidate years to simulate within these periods, we began with projections of future precipitation which then drive the river model. Projected changes in precipitation are addressed in detail in Caesar and Janes (2018) and Caesar et al. (2015): they conclude that "while the number of wet days is projected to decrease, the intensity of rainfall on these days is projected to increase, which could imply an increased risk of flash flooding, and an alteration to freshwater availability across Bangladesh". In order to integrate these changes into a value to guide our scenario choice, we next analysed the river discharge volume rates from INCA (Whitehead et al., 2015b).

Cumulative river discharge was used to guide the selection of scenario years: for a mid-century period (2030–2059) and a late century period (2070–2099). Temperature and precipitation forcing comes from the Met Office Hadley Centre HadRM3P RCM for South Asia, using three realisations: Q0, Q8, and Q16, to represent uncertainty associated with the climate model. All river discharge years from these climate realisations were examined, and those with maximum/minimum cumulative annual discharge were selected to be simulated in FVCOM. The shape of the hydrographs can be variable from year to year, which will have an impact on the arrival time of freshwater. As the GBM catchment covers many different environments, different stretches of the river may respond differently to future climate forcing. For example, the Brahmaputra has a much longer high flow period linked to snow and ice melt, while the Ganges has a relatively short high flow period (Whitehead et al., 2015b). The Meghna has much lower total discharge, but responds more strongly to local precipitation during the wet season. This is an area for further study, and will impact the exact timings of salt intrusion and freshening. We use these bounding years as our scenario forcing, as we are interested in the likely range of future conditions rather than examining behaviour in a single year. The daily and cumulative discharge volume for each scenario year used is shown in Table 2. Scenario S1 represents a baseline condition consistent with present day flows. Scenarios S2 and S4 represent years with the largest cumulative volume of freshwater, and scenarios S3 and S5 relatively low cumulative river discharges. It is important to note here that while those years chosen to represent particularly wet conditions have a high cumulative discharge and wet season flow, they can also experience particularly low flows in the dry season months. In this case we will describe scenarios S2 and S4 as 'extreme' futures, and S3 and S4 as 'moderate' futures. In addition to changes in total river volume discharged during the year, it is also important to consider the nature of freshwater input and tidal influence. The timing and intensity of freshwater input is closely related to the timing and intensity of the monsoon as illustrated by the left hand

Table 2
Total river discharge volumes in m^3 (summed over three month periods) used to drive future model scenarios. The river discharges come from the INCA catchment model, and details of the climate and management strategies can be found in Whitehead et al. (2015a). The more extreme years (scenarios 2 and 4 have significantly wetter wet seasons, and slightly drier dry seasons. Scenarios 3 and 5 have a cumulative discharge closer to that seen in the baseline simulation (compare with Fig. 1.).

Scenario	Mar–May	Jun–Aug	Sep–Nov	Dec–Feb
historic	10.952.76	58,585.75	28,623.27	5523.29
1	20,964.46	40,964.25	37,223.37	3913.06
2	14,892.47	71,262.06	61,888.19	4141.17
3	25,093.28	43,541.88	32,512.92	4915.36
4	12,863.70	88,414.26	76,083.48	3487.37
5	17,378.44	58,536.86	35,781.71	8384.66

panel of Fig. 2 which shows the daily river discharge entering the model. In 'extreme' years (blue and green curves) there is an early and sharp monsoon onset around the middle of July (day 200). A more gradual and later onset (around day 220 – early August) occurs during the two 'moderate years' (pink and red curves).

Having chosen these extreme climate states, a corresponding SLR was applied at the ocean boundary for consistency. SLR is included in the model through the open-ocean boundary, by raising the total water level, and this mechanism is discussed further in Kay et al. (2015). The SLR scenarios were based on the central estimate of SRES scenario for A1B (Church et al., 2013). To put this in context of more recent emissions and warming scenarios, the projected SLR for A1B lies between RCP4.5 and RCP8.5 for 21st century. The mean SLR for each scenario year is presented in Table 1. The sea-level will also have impacts on tidal dynamics in the region which is addressed in section c.

4. Results

4.1. Present day river salinity

The northern Bay of Bengal and coastal Bangladesh experience a strong horizontal gradient of salinity, varying from 0 to 35 in the space of 100 km see e.g. Rao and Sivakumar (2003). Although limited in situ observations of inland salinity are available. Dasgupta et al. (2014) present river salinity observed at 34 sites in coastal Bangladesh. Even with this limited data, a clear spatial pattern emerges, with a strong longitudinal gradient, with the highest salinities ($>$ 30) in the west, and fresher river waters ($<$ 2) in the east. This is because the majority of the freshwater discharges through the eastern distributaries, especially the Meghna Estuary, and the western delta is composed mainly of tidal creeks with little or no freshwater input. However this broad pattern does not capture the complex pattern of river salinity in the delta system, which is controlled by channel connectivity and a competition between river discharge and tidal hydrodynamics.

Until recently, the implications of climate change for saltwater intrusion in Bangladesh have not been much investigated (Bangladesh Bureau of Statistics et al., 2009). There is an inventory of river salinity observations held by the Bangladesh Water Development Board (BWDB). This covers 26 sites, with some observations from the early 1980s. The BWDB data consists of electrical conductivity measurements. Since around 2000 there have been monthly observations at least 16 sites, although at other sites data are only recorded during the dry season. An updated list of all available data is held online at http://www.hydrology.bwdb.gov.bd/.

To address this gap in the data, a new set of observations has been collected by Jahan et al. (2015). As well as salinity, other water and soil quality parameters were also recorded for the Southwest coastal region of Bangladesh. Maps of water pH, salinity, sediment concentration, etc. can be found in Jahan et al. (2015). Their study (undertaken in parallel to the modelling work presented here) is also a part of the "Assessing health, livelihoods, ecosystem services and poverty alleviation in populous deltas" under the Ecosystem Services for Poverty Alleviation" (ESPA) programme. 334 river water samples were collected during February 2014 to May 2014, providing us with a more detailed spatial picture of salinity in the GBM delta.

These observations of dry-season salinity can be used as a validation dataset for the FVCOM salinity model configuration. Fig. 3 (left panel) shows modelled mean salinity for March–May 2000 with scatter points of the sites where salinity was observed (Jahan et al., 2015) overlaid. From this figure we can see that the model is capturing well the spatial pattern of river salinity, with a strong lateral gradient observed from north east to southwest. The full range of salinities is captured, with near fresh (less than 0.5) waters seen in the lower Meghna, and high salinity waters close to ocean salinity ($>$ 34) in the south west of the delta.

Fig. 3 (right panel) shows a scatter plot of Model Bias to assess the performance of our numerical model. Model Bias is defined as $S_{obs} - S_{mod}$ where S_{obs} is the observed salinity, and S_{mod} is the modelled mean salinity during the period March–May. Overall the root mean square (*rms*) error with respect to observations is 6.98. The spatial distribution of the observed salinity is well captured in the model. Over the majority of sites the modelled salinity is slightly too fresh, with a median absolute error (*mae*) of 3.12. This bias is mainly homogeneous across most of the delta, apart from a section around 89.5 E (in the WES) which stands out with a larger fresh bias. Any disparity between the spatial patterns from model and observations may be due to problems in channel connectivity in the model. In our model configuration, freshwater is introduced at a single point, and allowed to redistribute through the channel network. The modelled year is forced by a climatology and is not a hindcast year, in this case modelled salinities are consistently lower than the observations. Even so, the spatial pattern is consistent, capturing the lateral salinity gradient ranging from 0 to 35 seen during the dry season. Even though a direct comparison cannot be made, the two results are correlated with an R^2 value of 0.76. Our simulation results also correspond well with the spatial patterns of modelled and measured salinity presented in recent work by (Akter et al., 2019). Therefore we are confident that the FVCOM model is able to capture the patterns of behaviour of the salinity distribution in the GBM delta.

4.2. Seasonal and tidal controls on salt intrusion

Next we look at the interactions between river and tide, and how they impact salt intrusion. Salt intrusion is a common issue for many

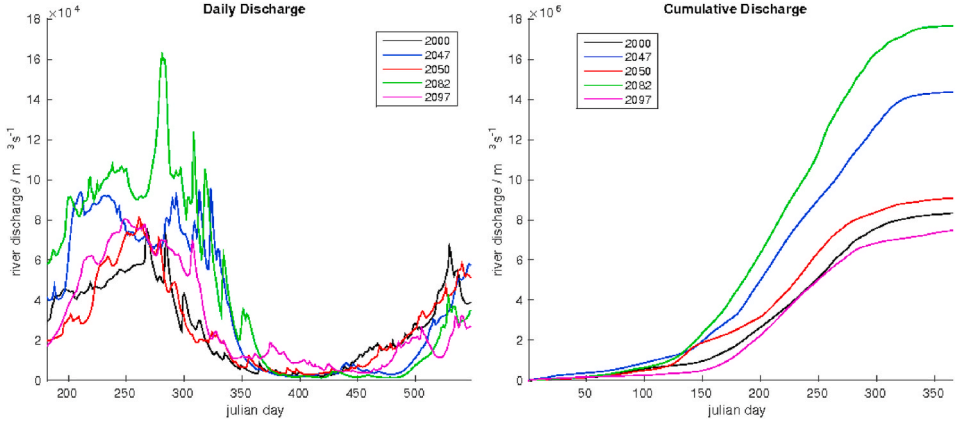

Fig. 2. Daily river discharge used as model forcing (left) and cumulative annual discharge (right) in (m^3) used to drive future model scenarios. The river discharges come from the INCA catchment model, and details of the climate and management strategies can be found in Whitehead et al. (2015a) The scenarios are run from monsoon to monsoon period, starting on 1st July each year.

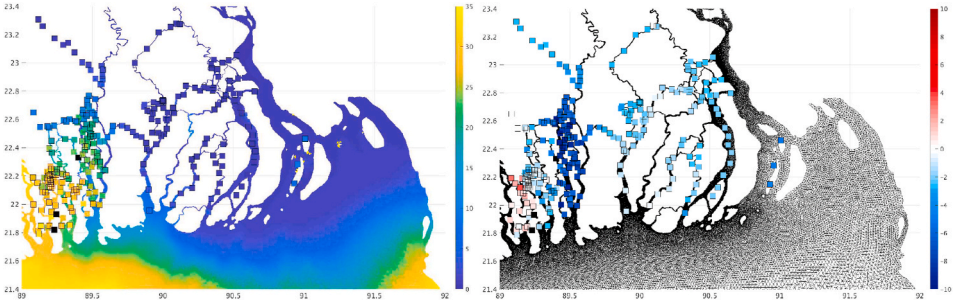

Fig. 3. Left panel: Mean modelled salinity during 2000 (left), overlaid with observed values (squares) between the period March to May 2014. Right panel: Model bias between observed values (instantaneous) and model average during the period March to May 2014. The observed salinity data are reproduced after Jahan et al. (2015).

large deltas, particularly where strong tides advect seawater long distances inland. Though we focus on the GBM, it is not unique in being a site at which these properties intersect. We are interested in understanding how tidal forces and seasonal freshwater interact to control the distribution of salinity in the delta and nearshore. The addition of a large volume of freshwater will increase water levels at all states of the tide. In our model, including freshwater as well as tide acts to increase mean low water (MLW), mean sea level (MSL), and mean high water (MHW) by just under 1 m at times of maximum discharge. The great diurnal tidal range (GT) which represents the difference between highest high water and lowest low water is seen to rise by 0.23 m on average across the model domain.

Increased river flow and changing tidal dynamics also affect flow patterns and current speeds within the delta. Peak flows in the Gorai regularly exceed 0.6 ms^{-1} in March, and 1.2–1.5 ms^{-1} in September. This may be compared with Rahman and Yunus (2016) who find depth-averages velocities exceeding 1.2 ms^{-1}. in the Gorai during wet season, while the Padma can flow as fast as 0.8 m^{-1} in March and exceed 2.2 ms^{-1} in September. These values are in line with the finding of Roy et al. (2016), who observe maximum flows in September of up to 1.8 ms^{-1}, and March 0.5 ms^{-1}. A detailed analysis of changing tidal dynamics is found in the appendix.

Fig. 4 shows seasonal mean salinity during the dry season (March) and post-monsoon (September). By taking a long term average, the effects of the tidal cycle are removed, and seasonal freshwater effects are revealed. In the dry season, with low discharge, higher salinities are seen to penetrate into the central section of the delta. The freshwater plume is also smaller in area, and remains close to the coast. With the increased discharge in September, the area of the freshwater plume increases (particularly waters with a salinity below 1). Though the large channels of the lower Meghna remain relatively fresh throughout the year, the salinity in the narrow channels in the central and western sectors of the delta is more strongly affected. Smaller river channels in the CES have an increased freshwater flow, and are also seen to freshen, extending the plume further to the west. Further offshore, away from the narrow river channels, freshwater enters the Bay of Bengal, and spreads out into a coastal plume. The freshwater plume creates a layer between 5 and 10 m thick in the vertical (not shown). The extent and position of this freshwater plume may have implications for coastal water quality, nutrient fluxes, and fisheries.

At shorter timescales, the tidal mixing and advection dominate changes in river salinity (Haque, 2006). Changes over the course of a single day can be large, and can alter local river salinity by as much as 10 during a 12.4 h semi-diurnal cycle. Fig. 4 indicates how much salinity can change locally over the course of a spring-neap cycle in the wet season. (This figure was generated by taking the largest and smallest salinities during a 48 h period in September). At the edge of the freshwater plume, a front is formed. Across the front there is a region where

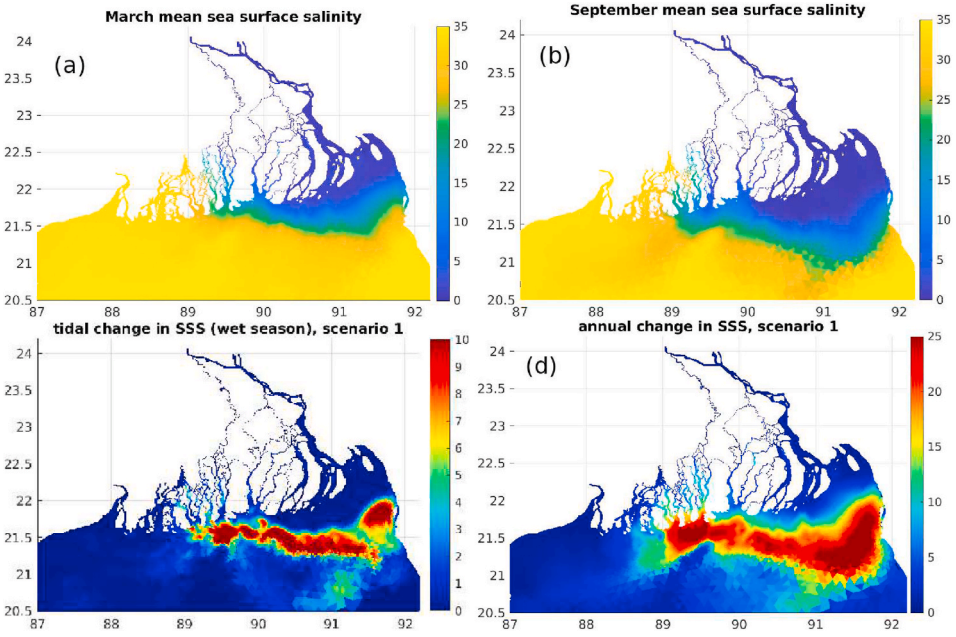

Fig. 4. Sea surface salinity (SSS) maps from scenario 1 (a) March mean salinity (b) September mean salinity (c) change in SSS over the course of 5th-6th September (d) change in SSS over the course of one year. NB change in colourscale between the lower 2 panels.

the water column becomes vertically stratified, with the freshwater plume overlaying seawater. Here tidal mixing is in competition with river run-off with the tides driving a well mixed water column, while stronger river discharge drives stratification. In the east, this front is 10s of km offshore, however the interface intersects with the coast in several places in the central estuarine section. Where the freshwater front is further inland, it will be important for irrigation waters to be extracted at the surface, as significantly saltier seawater will be present at depth. The largest changes in local salinity occur along the sharp front, where tidal forcing controls salt intrusion length. Further inland the impact of the tide is also observed, particularly in the WES and channel mouths of the Sundarbans. In the eastern estuarine section (EES) and Meghna, the tidal excursion is still large, but the waters here are so fresh that no local change in salinity is observed. The equivalent map for a seasonal cycle is shown in Fig. 4d, which shows the change in local salinity over the full year. These changes can be three times as large as the tidal effects, and act mainly at the front of the freshwater plume. However, a strong sensitivity to the seasonal change in freshwater flux is observed in the WES, as far as 22.5 °N. The WES is particularly sensitive to both tidal and seasonal excursions while in the CES and EES, the freshwater plume extends further offshore.

As well as tidal and river forcing, dynamics may be further influenced by the Earth's rotation. In the south east of the delta, river channels can be of the order of 10 km wide. Here (if the waters are stratified) rotational effects can become important. However, the waters are mostly well mixed in the vertical. At the edge of plume (where waters are stratified) rotational effects may become important; here the first baroclinic Rossby radius is of the order 500 m–2 km. However these effects will also be negligible in the well mixed and narrow channels of the river delta. When close to the coast and in shallow water, friction can become important as well as tides, freshwater, and rotational effects. The frictional impact on the tides is discussed further in the appendix.

Another seasonally varying metric is the flushing time (T_f), which can be thought of as a time in which to flush all salt out of the system. The flushing time of an estuary is defined as the time needed to replace its freshwater volume V_F at the rate of the net flow through the estuary, which is given by the river discharge rate Q ($T_f = V_F / Q$).

As an indication of spatial variability in flushing time, we calculate T_f for the 3 sections. In the wet season around 83% of water flows through the EES, 7% through the CES, and 10% through the WES. In the dry season, this changes to 91% EES, 8% CES, and just 2% through the WES. Combining this with measures of the corresponding model grid areas, T_f can be calculated. In the WES, the shortest flushing time in the wet season is 44 days, 21 days in the CES, and just 3 days in the EES. These values can be recalculated throughout the year, and change by up to two orders of magnitude. However with a transient behaviour to changes in river flow, these static estimates of flushing time are not really meaningful in dry season. Nonetheless, this does give some indication of the very different river influence in different section of the GBM delta.

4.3. Future changes in tidal and hydrodynamic behaviour

An analysis of present day tides in the GBM delta was performed in Bricheno et al. (2016), assessing the performance of the FVCOM model in this area. This previous study focused on the performance of the model for representing tidal and river water levels, for a historic period. In the present work, we assess the future changes, in climate-model driven scenarios. As a measure of how SLR affects tidal hydrodynamics, we consider changes to the tidal range, and how it is amplified when moving from deep water onto the shelf and into river channels. The amplification is defined as $\frac{\text{range}(i)}{\text{range(Shelf Break)}}$ and is calculated at every point (i) throughout the model. As a measure of tidal energy dissipation, u_b^3 is also evaluated. where u_b is the bottom velocity; again this is calculated at all points within the model domain. Fig. 5 shows the

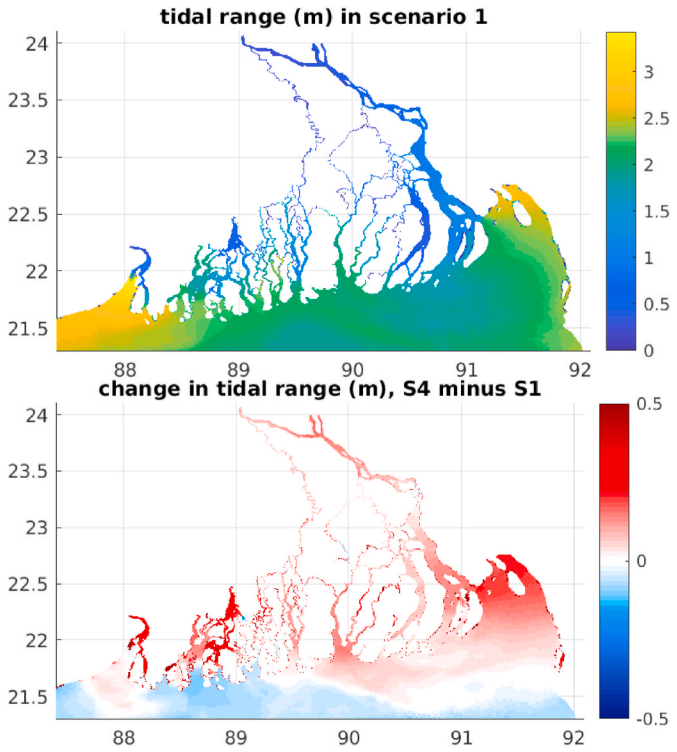

Fig. 5. Tidal range (m) in scenario 1 (top), and below: difference in tidal range (m) between scenario 4 (mean sea-level rise 0.5877 m) and scenario 1 (no sea-level rise).

difference in maximum tidal range for scenarios 1 and 4. This comparison should represent the largest projected change, as it included the largest range of discharges, and a large SLR by the end of the century. The changes are subtle, but significant (differences in tidal amplitude of the order 0.5 m). An increased tidal range is seen at the mouth of the Meghna in the east and in parts of the Sundarbans. The largest increases are well correlated with the sites of largest tide, suggesting a consistent increase across the northern Bay of Bengal. Within the delta, differences are largely positive with a mean increase of 0.40 m, but the changes vary between a reduction in range of 0.73 m, and an increase of 1.8 m. The greatest increase in range is predicted to occur in the Sundarbans, and the Hooghly river in India.

When the full simulations are assessed (including freshwater as well as tide), water levels are seen to increase across all states of the tide. Mean low water (MLW), mean sea level (MSL), and mean high water (MHW) are seen to rise by just under 1 m. The great diurnal tidal range (GT) which represents the difference between highest high water and lowest low water is seen to rise by 0.23 m on average across the model domain. The means are presented in Table 3, and have been spatially weighted to avoid skews introduced by the unstructured nature of the model mesh. A caveat to this is that a large positive increase may be associated with increased river discharge raising the water levels. A further discussion of this, and map of sites where river discharge impacts total water level are shown in the appendix.

A harmonic analysis was performed to derive the tidal constituents at 105 points across the delta (a selection chosen to represent all possible tidal conditions), using the T-tide package for Matlab (Pawlowicz et al.,

Table 3
Changes in spatially averaged tidal water levels (m) between two scenarios.

scenario	MLW	MHW	MSL	GT
S1	0.18 m	1.91 m	1.02 m	3.22 m
S4	1.13 m	2.83 m	1.95 m	3.45 m

2002), and the locations are plotted in Fig. 1. Fig. 6 shows how tidal amplitudes change under increased sea level and variable river flow. When analysing the tidal harmonics, a modest change is seen across the four leading constituents (M2, S2, K1 and O1). M2 amplitudes are seen to change by of the order 0.1 m in S2 and S3, but are consistently larger in scenarios S4 and S5 by circa 0.2 m across the delta. S2 sees a similar trend, with all future scenarios increasing in S2 amplitude by around 0.1 m at all the sites analysed. Turning to the diurnal constituents, a modest increase in amplitude of the order 0.02 m is observed across all future scenarios, at all sites. Though on average tidal ranges will increase under future scenarios, the maxima are largely unchanged. The semidiurnal constituents are largest in the two 'corners' of the Bay of Bengal, to the north west and north east. Here, the largest absolute increases in M2 and S2 amplitude are observed in future projections. The diurnal constituents are seen to increase in amplitude, with the largest increase seen in the eastern estuarine section (north east Bay of Bengal) of by 0.02–0.03 m in places. The closest amphidromic point is located near Sri Lanka (far outside of our model domain). In the future simulations, the co-tidal chart of e.g. M2 is very similar, suggesting little change in amphidromic position in our model. Further discussion on changes in tidal dynamics in response to climate forcing can be found in the appendix.

4.4. Future changes in salinity

Fig. 7 shows the mean salinity during March (left) and September (right) for all five scenarios (S1 top to S5 bottom). In these plots the unstructured model data has been interpolated onto a regular grid, in order to fill-in the gaps, and give an impression of surface salinity across the delta. The coastline has been highlighted in white for orientation. It is important to focus on a small range of salinity between 0 and 5, and the non-linear colour scale has been expanded to highlight this range. As a reminder, the critical contours for drinking water (salinity = 1) and irrigation water (salinity = 2), while mangrove forests are most productive at salinities between 2 and 9 (Ye et al., 2005).

The March plots (left column) represent the dry season, so the freshwater plume is smaller and close to the coast. In the future projections it can be seen that the freshest contour lines shift further in-land in all scenarios. This represents increased salinity intrusion in all futures. Higher salinities in the future are seen particularly strongly in the CES. In the WES the onshore-offshore salinity gradient is largely unchanged, with high salinity waters (above 10) seen across the Sundarbans mangrove forest. In the EES, salinities are seen to remain below 5 in future. This shows the CES (89.5–90.5 °E) is the most sensitive to dry-season salinity intrusion in future projections.

Next, let us consider the mean salinity during the wet season (September), in the right-hand column of Fig. 7. Here we see contrasting results in different areas of the delta. In the EES there is a larger area of freshwater in all future scenarios, with the river plume extending further offshore. There is little change in the WES, with waters remaining about 10 throughout September. The largest inland changes are observed in the CES, where an increase in salinity is observed in all future scenarios. This salt intrusion can be as large as 5 in places, and is at its most severe in S4 and S5 (the years with the largest SLR). This is an interesting result, as looking back to the projected river discharge (Fig. 2) suggests a similar discharge in S3 and S5 (the moderate years) to the baseline S1, while S2 and S4 (the extreme years) have significantly larger discharge during September.

The seasonal changes are clarified by plotting difference between each future and the baseline scenario (shown in Fig. 8). Similarly to Fig. 7, the left hand column shows March and the right-hand column

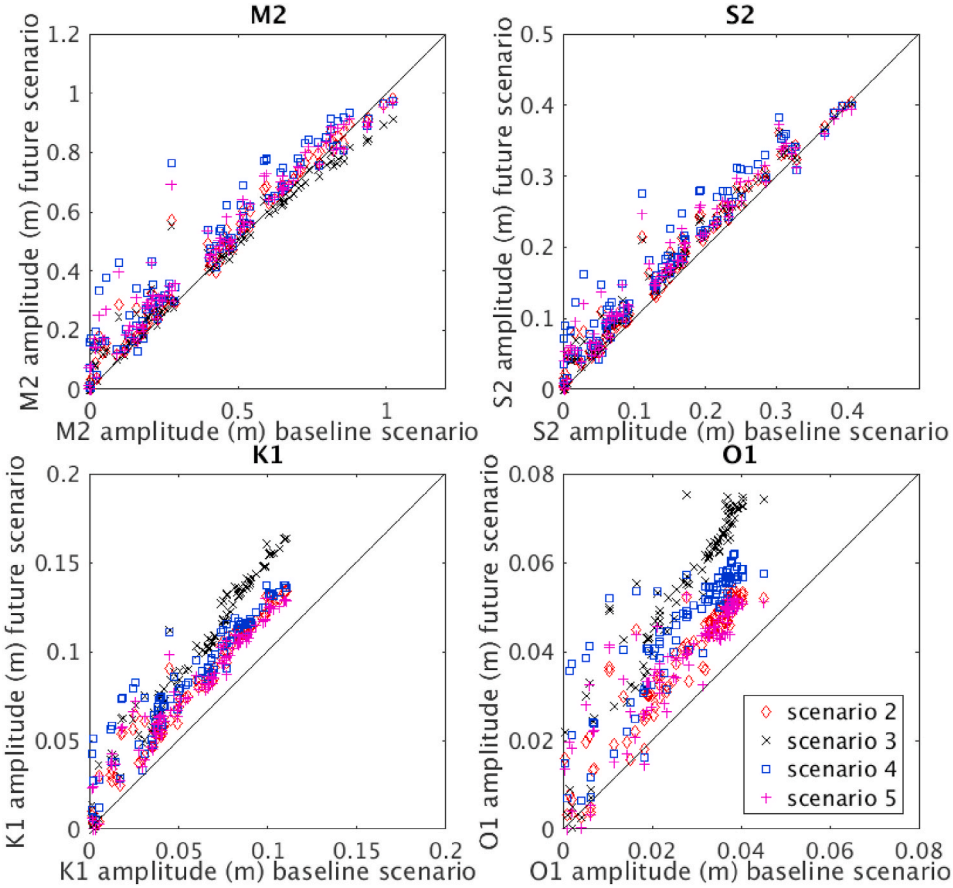

Fig. 6. Tidal amplitude of the four leading constituents at a selection (105 points) of sites within the delta. The four future scenarios defined in Table 1 are plotted against the baseline. the 1:1 line is added in black for reference.

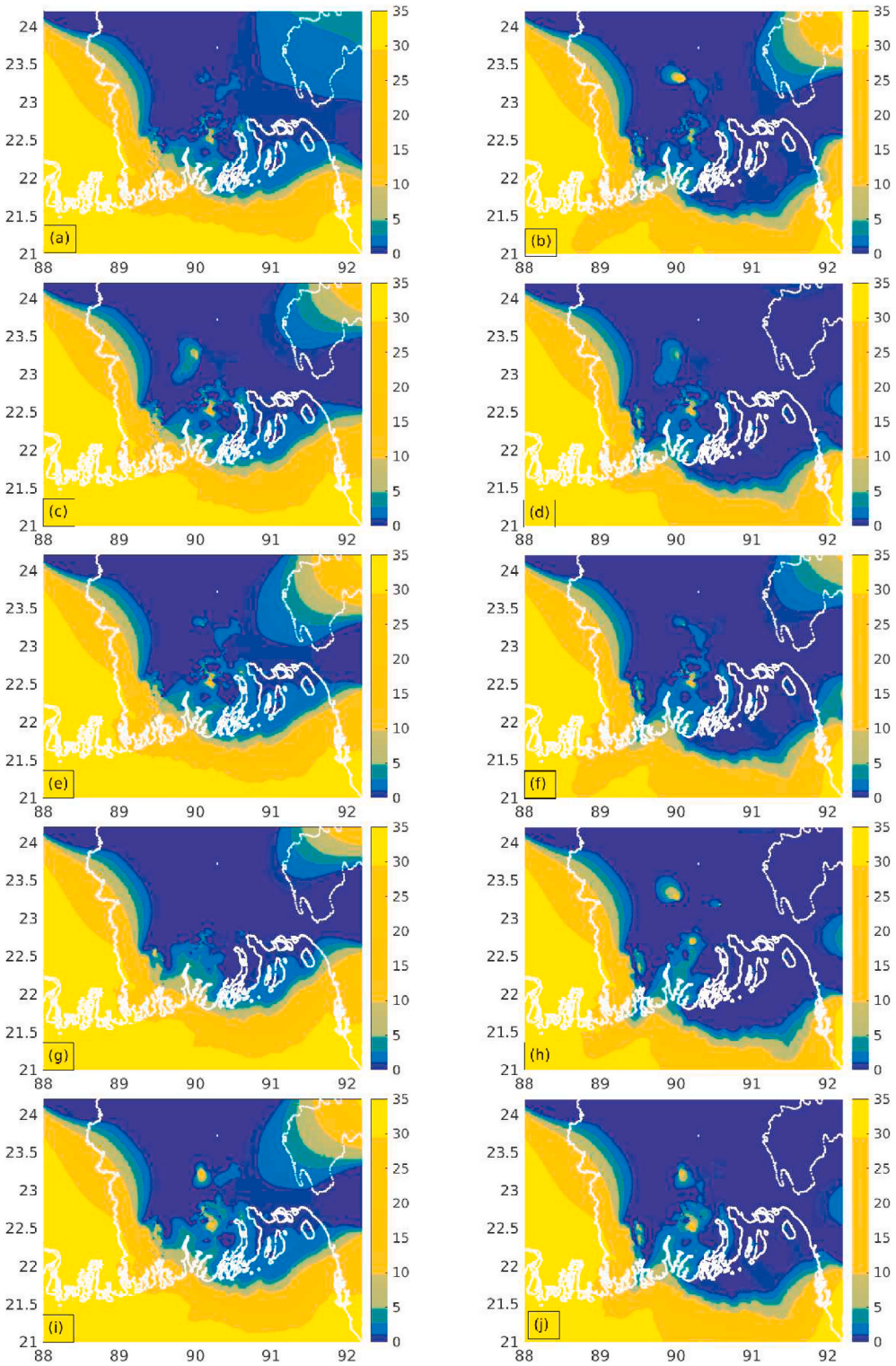

Fig. 7. Monthly mean surface salinity during each of the 5 scenarios, contoured to highlight critical thresholds. March (left) and September (right) from S1 (top) to S5 (bottom).

shows September. These maps confirm the picture of higher future salinity across coastal Bangladesh during the dry season. The average increase can be as large as 5 or more during March in these projections. All futures see higher maximum values in the WES and CES when compared with the baseline year, while the EES remains largely unchanged. The highest increases in salinity (observed in the central estuaries) can be as large as 10. For September, we can now clearly see the 'dipole' across the delta, with an increased salinity in the WES and CES, and a reduction in the EES around the mouth of the Meghna. The boundary at which this change map flips from positive (salt intrusion) to negative (freshening) is different in each future scenario. The location of this boundary may be the critical factor on the ground for indicating the changing water resource. This confirms that the CES is indeed the most sensitive area to future climate change.

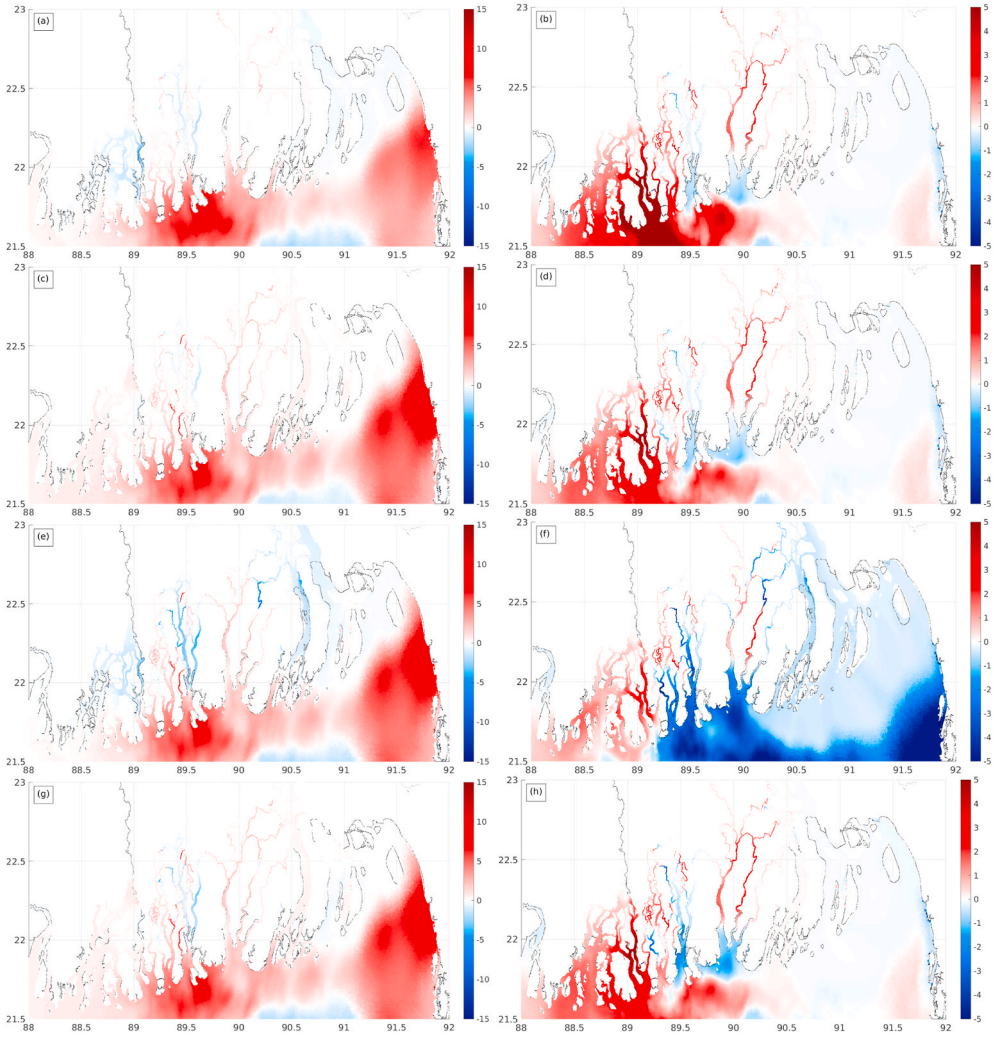

Fig. 8. Difference in monthly mean salinity (minus baseline) for all scenarios: March (left) and September (right) from S2 (top) to S5 (bottom).

To understand the causes better, we return to the changes in river and ocean forcings: altered discharge and SLR. Table 1, shows that the total annual river discharge is projected to increase in all scenarios. The mean flushing time (defined in section c) is reduced in future from 102 days in the baseline simulation to 93 and 86 days in the moderate years (S3 and S5), and 59 and 48 days in the extreme years (S2 and S4 respectively). The minimum flushing time (representing wet season flows) is also reduced, from 32 days in the minimum (fastest discharge) S1 to around 28 days in the moderate years (S3 and S5), and even shorter in the extreme years (S2 $T_f = 24$ days, and S4 $T_f = 14$ days). In other words, a shorter flushing time is predicted in all future scenarios, associated with higher discharge in future projections.

Table 1 shows that, even though the projected discharge is seen to increase in all scenarios, the surface salinity is much higher across much of the delta. It is important to notice that, though all future scenarios see an increase in river flow, in some places the surface salinity is still seen to rise. As we are not including a (meteorological) surface freshwater flux in the model, the only possible mechanisms controlling river salinity are (1) penetration of seawater into the delta due to SLR and (2) freshening locally due to higher discharge. There may be also changes in the characteristics of the incoming sea-water salinity, so this variable needs to be included in our analysis. To investigate whether there is a change in ocean conditions, we can look at salinity evolution at the open boundary of the model. Table 4 shows the mean salinity in the forcing model GCOMS at 19 °N, which is used to drive the FVCOM model. The figures in Table 4 indicate that ocean salinities are very similar at the ocean boundary, i.e. we are not imposing a salinity change at the open-ocean boundary. Therefore we can discount changing ocean salinity as a driver for higher future river salinities in the delta. This suggests that any projected increase in river salinity must be controlled by hydrodynamics (moving high salinity ocean water inland) rather a change in the

Table 4
Ocean salinity forcing for modelled scenarios.

Scenario years	Mean 'ocean' salinity
2000–2001	34.39
2047–2048	34.10
2050–2051	34.38
2082–2083	33.99
2097–2089	34.22

Table 5
Excursion of the salinity = 15 contour at 91 ° East on a tidal and seasonal timescale.

Scenario	years	tidal excursion	seasonal excursion
S1	2000–2001	12.1 km	65.6 km
S2	2047–2048	12.0 km	63.5 km
S3	2050–2051	13.1 km	60.3 km
S4	2082–2083	11.1 km	68.5 km
S5	2097–2089	12.7 km	63.7 km

offshore salinity. We have observed in section (c) that SLR altered the hydrodynamics in this area (see Table 5). Higher MSLs and changes in tidal conditions are bringing more ocean water further inland. This process contributes to an increase in river salinity on the delta, overriding changes in river discharge. We conclude that the increased salt intrusion is caused mainly due to rising sea levels. Ocean processes bringing salt-water inshore are more dominant in future, even when river discharge is significantly increased in future projections. However, the SLR effect is enhanced or in some cases only slightly mitigated by changes in river discharge.

Having mapped the areas at risk to changing salt intrusion, we can also examine how the tidal and seasonal excursion of salt intrusion length change in the future. Table 4 shows the typical distances a modelled contour of salinity moves under a tidal and seasonal cycle. The seasonal excursion is around 5 times the distance of the tidal excursion for all scenarios. At this example site, there is a change of around 1 km, or 10%. So although the positions of critical contours are subject to future change, the seasonal and tidal excursion lengths do not seem to be so sensitive. There may be some sensitivity related to the interactions between SLR, tides, and storm surge. For example Akter et al. (2019) note that an increased tidal range can generate stronger salt intrusion during the cyclone events.

4.5. Future changes in freshwater resource

Section d demonstrated how the salinity of local surface water may change in the GBM under future climate projections. It is also important to understand how potential changes in future wet/dry seasons will affect the availability of freshwater, and productivity on the delta. Two important factors for crop irrigation waters, are (1) the date of freshwater arrival, or onset of monsoon, and (2) the length of time for which waters are fresh enough for irrigation use. The arrival of freshwater in different areas of the delta will be controlled strongly by inland ice melt, and the onset of monsoon rains. This will constrain timings and shape of the river hydrograph. The discharge plots (Fig. 2) gives some indication of how changing monsoon conditions impact river flows, suggesting an earlier onset and longer duration during wet years. However, the subsample of experiments performed here were based on extremes of cumulative freshwater. Therefore we may not represent the full range of possible future river discharge profiles. Further work to understand the impact of climate change on hydrograph shape is desirable. While we cannot determine specific dates, we are able to investigate the length of the growing season, and how these windows may evolve under climate change. Bangladesh has three rice seasons, the aus, aman, and boro. The aus or summer rice crop is planted during March–April and harvested during June–July. The aman season rice is planted in June–July and

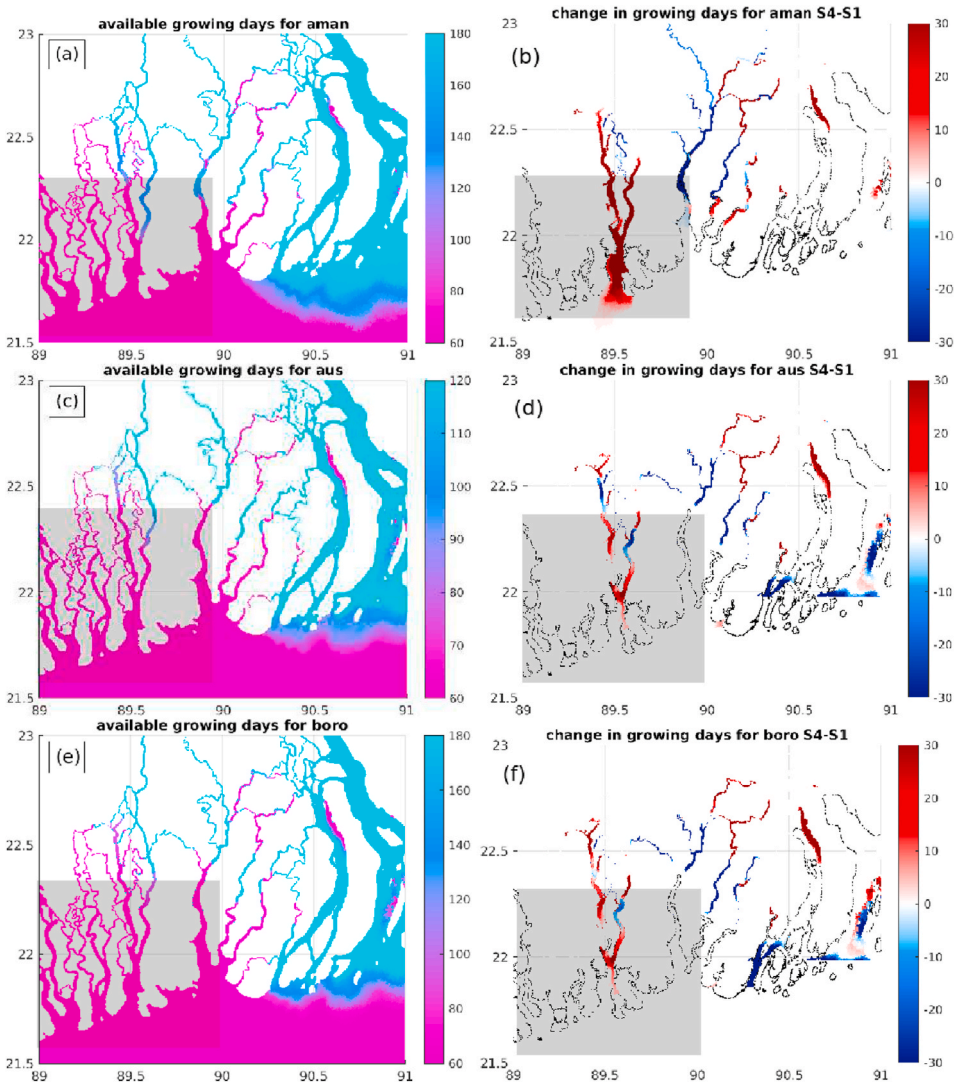

Fig. 9. Number of growing seasons per year in S1 (left) and change in growing seasons S4 minus S1 (right). Note that changes in offshore waters south of 22 °N have been masked out. The Sundarban forest (where there is no rice agriculture) is also covered with grey shading.

harvested during November–December. The boro season rice is planted in December–January and harvested during May–June. BBS (2017). Aman rice is the most important staple food, and due to the monsoon rains, it requires minimal irrigation. Boro rice on the other hand requires irrigation during the dry winter period (Clarke et al., 2018). By examining these growing seasons, and the changing number of days within each period, we can see how salt intrusion may impact on agricultural productivity in the delta.

Fig. 9 shows the number of days per season where surface waters are suitable for irrigation. For blue areas, the surface waters are fresh enough to use throughout each growing season. In pink areas, the salt intrusion is too large for a viable crop. The right hand panels show the change in number of 'fresh' days per season, comparing S5 and S1. There is a reduction in freshwater availability in the CES for all seasons, particularly strongly in the aman season, with a shortening of 30 days in places. The salt intrusion shortens the growing season in the EES and CES for all three seasons. Some areas see an increase in fresh days (coloured red), however these are at sites where the growing season is already too short for viable cropping (for example in the central estuarine section 22 °N, 89.5 °E).

By assuming a minimum growing season of 120 days, following the guidelines of Saha et al. (2015), we can make a crude calculation of how this will impact yield across the delta. To do this we count the locations where there are 120 fresh days per season, and then compare this as a percentage with the historical baseline. Then take a mean value across all locations in the model domain. This gives an indication of what fraction of the delta can support each rice crop compared with present day conditions. Table 6 shows these fractions for all three rice cropping seasons for 4 future scenarios compared with the baseline.

In almost all combinations of crops and scenarios, the potential growing time is seen to reduce. No one season seems more sensitive than the others in this compound measure, but these values must be considered in the context of the spatial distribution mapped in Fig. 9. The strongest impacts on growing season length are seen inland, with a reduction of up to 30 days in the CES for S4 and S5 (maps for all scenarios not shown). For example, Fig. 9 shows that the reduction in aman season in the CES makes this crop no longer viable in S5. To summarise, the drier futures experience a reduction in the length of the growing season over a significant area of the delta. The change in time for which freshwater is available can be reduced by more than 10 days on average days in some projections. The most extreme impacts are seen in scenarios 2 and 5.

There are multiple agricultural land uses in the GBM delta, including subsistence rice, commercial rice, brackish shrimp, and vegetable crops. Changes in the local water quality will impact farming practices and in turn the wellbeing of people living on the delta (Nicholls et al., 2016). As well as impacting this agricultural productivity, salt intrusion will also affect the Sundarbans mangrove forest. Several mangrove tree species reach an optimum growth at salinities of 5–25% of standard seawater (Ye et al., 2005), and are therefore also sensitive to changes in seawater intrusion. This equates to a range of salinity between 1.75 and 8.75. A detailed study of the projected impacts of climate change on the mangrove extent in this area are found in Payo et al. (2016).

Table 6
Projected change in growing seasons: change in percentage of time and number of days where irrigation water is viable.

Scenario	aman %	boro %	aus%	aman days	boro days	aus days
S2	93.9	92.8	92.9	−10.9	−12.9	−8.5
S3	97.8	99.8	97.9	−4.0	−0.4	−2.5
S4	99.9	98.5	98.6	−0.2	−2.6	−1.7
S5	93.9	94.7	91.6	−10.9	−9.6	−10.1

5. Discussion

River salinity on the GBM delta is controlled by a balance between monsoonal freshwater discharge flushing salt offshore, and tidal hydrodynamics pushing seawater inland. By decomposing the movement of the freshwater front into a tidal and seasonal timescale, we can identify which areas will be most sensitive to changes in tidal and river forcing. Experiments have been performed using climate and SLR forcing to understand future salt intrusion in the GBM delta. We predict an increase in mean tidal range throughout the delta caused by a combination of reduced river discharge and SLR. Recent work by citepakter2019dominant uses Delft3D to simulate surface water salinity in Bangladesh, under different climate conditions. Similarly to our study, they find that a reduced river discharge causes increased salt intrusion across the GBM delta. However, with SLR scenarios of 0.25 and 0.5 m, they observe no additional salt intrusion to the delta, which is contrary to our study. In the highest SLR scenario of 1 m, they project that salinity will increase, but the impact is restricted to the shallower coastal zone. They also go on to study the impact of cyclones on salt intrusion, which may be a direction for our further work.

Larger tides and rising MSLs lead to increased tidal penetration and salt intrusion. Though there is little change in ocean salinity offshore in the future projections, the tidal hydrodynamics are able to drive the salty 'ocean' water further inland than in the recent past. As well as affecting the salinity of river water, the movement of this salinity 'front' will likely also impact upon the salinity of the groundwater (Werner and Simmons, 2009). Sherif and Singh (1999) project that a SLR of 0.5 m in the Bay of Bengal will cause an additional increase in sea water intrusion of 0.4 km. It is hard to put a single number on this salt intrusion over such a complex river system and this should probably be considered on a channel by channel basis. During the dry season we project an increase in salt intrusion of around 10 km (Fig. 7) when considering the position of the 2 PSU contour. However the movement of this front is not coherent. Examining other thresholds, the contours can shift by as much as 0–90 km, depending on the chosen value, and the maps are complex.

In the future, we see higher river discharges, but the impact of this change is restricted mainly to the EES. This increased discharge is enough to counteract the influx of sea water from rising sea-levels in the east, keeping future river salinity here relatively unchanged from the present day. In the WES, historically salinity values are high, and remain so in future projections. The CES is the most sensitive, as it is this area where strong salinity fronts currently exist. Here the position of the front is critical, and salinities are projected to rise the most in future, particularly during the dry season where it can increase by over 10 in places (Fig. 8). This area is also the most critical for irrigation, as the land use here is predominantly agricultural.

In the future, a more extreme climate is projected for South Asia, with drier pre-monsoon and wetter monsoon seasons (Fig. 2). This shows the importance of analysing future projections seasonally, with a focus on increased salt penetration in the dry-season. Future scenarios project a delay in the arrival of irrigation quality river water, as well as a change in the duration of the growing season, the length of time for which freshwater is available for irrigation.

Clarke et al. (2015) assert that dry season irrigation water is likely to become more saline by the end of the 21st century. Our results support broadly this claim, while giving a more detailed spatial pattern to the projection. We have demonstrated the impact that salt intrusion may have on crop production, and potential impacts on subsistence livelihoods and well-being. A link between salinity and poverty has already been made by Johnson et al. (2016a), who present spatial maps of poverty in this area, stating an "increase in levels and intensities of salinity in a union increases the probability of the union being poor", i.e. areas of high salinity, especially in the western estuarine section are strongly correlated with those districts experiencing the worst asset poverty.

As well as affecting crop production, and native forests, future river

water salinity will impact on local soil, and groundwater salinity. The complex numerical model described in this work has contributed to an emulator model (Lázár et al., 2015; Nicholls et al., 2016). In the latter model, river salinity is modelled based on a linear relationship between river discharge and ocean water level, and informs water quality and agricultural productivity models. The salinity projections made in this work have also informed a soil salinity model described in Payo et al. (2017), and work on the future of the mangrove forest by Payo et al. (2016).

While most of our conclusions here relate to irrigation waters, we also make projections of the position of the salinity = 1 contour, which is the threshold for safe drinking water. The authors acknowledge that salinity is only one aspect of safe drinking water, and should be considered in the context of other water quality parameters such as arsenic, sewerage and pollution. Water quality and local salinity are not synonymous, but closely related (Nahian et al., 2018). Water quality could be related to nutrients and other pollutants, but here it is mainly controlled by salinity. The future salinity projections made in this work could also point to changes in nutrient pathways, and the fates of pollutants and heavy metals. There is scope for future work related to tracer pathways and nutrient cycling in the delta, using the unstructured modelling approach.

While our specific conclusions are drawn from the GBM delta, they have implications for similar tide-dominated deltas, where SLR can increase tidal range, and therefore exacerbate salt intrusion. For example De Dominicis et al. (2020) predict tidal amplification in the Pearl River Delta due to SLR. similar findings are reported by Nhan (2016) in the Mekong and Gong et al. (2012) in the Yangtze. This can be put into the context of an acceleration of the hydrological cycle in future climate (e.g. citekundzewicz2008climate). As many estuaries which already experience salt intrusion, are likely to suffer from decreasing water resource due to climate change reducing river flows and groundwater recharge. From a global perspective, we may expect similar responses to salt intrusion in other tide-dominated deltas, when SLR can override can seasonal river discharge.

6. Conclusion

River salinity in the GBM delta can be simulated with a variable resolution hydrodynamic model. The model presented here is capable of capturing both tidal and seasonal timescales. Salt intrusion has a pronounced spatial pattern, with the saltiest river waters observed in the western estuarine section and the Sundarbans forest. Waters become progressively fresher moving towards the east, and the mouth of the lower Meghna. There is a strong seasonal signal in the freshwater distribution controlled by large river discharge during the monsoon including within the freshwater plume which alters size, position and vertical structure throughout the year. Tidal excursion of the freshwater front can alter local river salinity by between 2 and 10 over the course of a day. River salinity is largely controlled by a combination of annual monsoon discharge and tidal processes.

A set of future scenarios were run to investigate the impact of rising sea levels and changing river discharge in the GBM delta. Altered freshwater input and ocean forcings affected the dynamics and crucially the salinity in the GBM delta. Under all future projections dry-season salinity is predicted to increase in the river channels. This increased salt penetration affects river salinity most strongly in the central estuarine section, in the region of the freshwater front. During the wet season, high river discharges in future climate scenarios enhance freshwater delivery to the delta, and can maintains low salinity at the mouth of the Meghna. In the eastern estuarine section, the increased river flow and increased sea level are more balanced, so there is little change in future salinity here.

We have demonstrated how SLR affects tidal dynamics, and in turn the excursion of the salinity front. Rising sea levels are concluded to be the most important factor controlling future river salinities in the GBM delta. The positions of the critical salinity contours (tipping-points for drinking water and agricultural productivity) have been projected for future wet and dry seasons, which shows that the central estuarine section (a marginal environment for subsistence farming) is most at risk from changing saline intrusion in the future. By extending projections of surface salinity into water resource availably, we have drawn conclusions about how climate change may impact on growing seasons and therefore productivity on the GBM delta.

Due to the interaction between SLR and changing river discharge in future projections the disparity between wet and dry season salt intrusion is seen to widen. In the future, rising sea-levels act to increase salt intrusion in the GBM delta. During the dry season, this effect is enhanced by reduced river discharge, leading to increased river salinity throughout the delta. In the wet season, the SLR effect is counteracted to some extent in the east by larger river discharge driven by an enhanced monsoon. However the central and western side of the deltas is dominated by SLR, leading to increased salt intrusion all year round. These conclusions (while drawn from the GBM delta) have implications for similar tide-dominated deltas, where SLR can increase tidal range, and therefore exacerbate salt intrusion.

Authorship statement

Lucy Bricheno: Conceptualization, Methodology, Software, Validation, Visualisation, Formal analysis, Investigation, Original draft preparation, reviewing and Editing, and Supervision.

Judith Wolf: Funding acquisition, Supervision, Conceptualization, Methodology, Investigation, Original draft preparation, reviewing and Editing.

Yujuan Sun: Software, Validation, Visualisation, Formal analysis, Writing- Reviewing and Editing.

Declaration of competing interest

The authors declare that they have no known competing financial interests or personal relationships that could have appeared to influence the work reported in this paper.

Acknowledgements

The ESPA Deltas project (Assessing Health, Livelihoods, Ecosystem Services And Poverty Alleviation In Populous Deltas), project number NE-J002755-1, was funded with support from the Ecosystem Services for Poverty Alleviation (ESPA) programme. ESPA is a collaboration between Bangladeshi, UK and Indian partners to develop a holistic picture of the GBM delta. The ESPA programme is funded by the Department for International Development (DFID), the Economic and Social Research Council (ESRC) and the Natural Environment Research Council (NERC) Project Code: NE/J002755/1. This work used the ARCHER UK National Supercomputing Service (http://www.archer.ac.uk).

Appendix A. Supplementary data

Supplementary data to this article can be found online at https://doi.org/10.1016/j.ecss.2021.107246.

References

Ahmed, Ali, Nahian, Mahin Al, Hutton, Craig W., Lázár, Attila N., 2018. Hypertension and malnutrition as health outcomes related to ecosystem services. In: Ecosystem Services for Well-Being in Deltas. Springer, pp. 505–521.

Ahmed, M Feroze, Ahuja, Satinder, Alauddin, Mohammad, Hug, Stephan J., Lloyd, Jon R., Pfaff, Alex, Pichler, Thomas, Saltikov, Chad, Martin, Stute, Alexander van Geen, 2006. Ensuring Safe Drinking Water in Bangladesh.

Akter, Rabeya, Zaman Asik, Tansir, Sakib, Mohiuddin, Akter, Marin, Sakib, Mostofa Najmus, Al Azad, A.S.M., Maruf, Montasir, Haque, Anisul, Rahman, Md, et al., 2019.

The dominant climate change event for salinity intrusion in the gbm delta. Climate 7 (5), 69.
Alcamo, Joseph, et al., 2003. Ecosystems and Human Well-Being: a Framework for Assessment. Island Press, Washington, DC, USA.
Allison, M.A., 1998. Historical changes in the Ganges-Brahmaputra delta front. J. Coast Res. 1269–1275.
Bain, R.L., Hale, Rip P., Goodbred, S.L., 2019. Flow reorganization in an anthropogenically modified tidal channel network: an example from the southwestern ganges-brahmaputra-meghna delta. J. Geophys. Res.: Earth Surf. 124 (8), 2141–2159.
Bangladesh Bureau of Statistics, World Bank, World Food Programme, 2009. Updating Poverty Maps of Bangladesh. World Bank Policy Research Working Paper.
BBS, 2017. Yearbook Agricultural Statistics 2017. Bangladesh Bureau of Statistics Dhaka, Bangladesh.
Biswas, H., Mukhopadhyay, S.K., Sen, S., Jana, T.K., 2007. Spatial and temporal patterns of methane dynamics in the tropical mangrove dominated estuary, ne coast of Bay of Bengal, India. J. Mar. Syst. 68 (1–2), 55–64.
Brammer, Hugh, 2014. Bangladesh's dynamic coastal regions and sea-level rise, 0 Clim. Risk Manag. 1, 51–62. ISSN 2212-0963. http://www.sciencedirect.com/science/article/pii/S221209631300003X.
Bricheno, Lucy, Wolf, Judith, 2018. Modelling tidal river salinity in coastal Bangladesh. In: Ecosystem Services for Well-Being in Deltas. Springer, pp. 315–332.
Bricheno, Lucy M., Wolf, Judith, Islam, Saiful, 2016. Tidal intrusion within a mega delta: an unstructured grid modelling approach. Estuar. Coast Shelf Sci. 182, 12–26. ISSN 0272-7714. http://www.sciencedirect.com/science/article/pii/S0272771416303791.
Brown, S., Nicholls, R.J., 2015. Subsidence and human influences in mega deltas: the case of the Ganges–Brahmaputra–Meghna. Sci. Total Environ. 527–528, 362–374. ISSN 0048-9697. http://www.sciencedirect.com/science/article/pii/S0048969715300589.
Caesar, J., Janes, T., Lindsay, A., Bhaskaran, B., 2015. Temperature and precipitation projections over Bangladesh and the upstream Ganges, Brahmaputra and Meghna systems. Environ Sci. Process. Impact. 17, 1047–1056.
Caesar, John, Janes, Tamara, 2018. Regional Climate Change over South Asia. Ecosystem Services for Well-Being in Deltas, p. 207.
Caldwell, Rebecca L., Edmonds, Douglas A., Baumgardner, Sarah, Paola, Chris, Roy, Samapriya, Nienhuis, Jaap H., 2019. A global delta dataset and the environmental variables that predict delta formation on marine coastlines. Earth Surf. Dynam. 7 (3), 773–787.
Cao, Yu, Zhang, Wei, Zhu, Yuliang, Ji, Xiaomei, Xu, Yanwen, Wu, Yao, Hoitink, A.J.F., 2020. Impact of trends in river discharge and ocean tides on water level dynamics in the pearl river delta. Coast. Eng. 157, 103634.
CEGIS, I., 2006. Lmpact of Sea Level Rise on Landuse Suitability and Adaptation Options. Center for Environmental and Geographic Information Services, Dhaka, Bangladesh.
Chen, Changsheng, Liu, Hedong, Beardsley, Robert C., 2003. An unstructured grid, finite-volume, three-dimensional, primitive equations ocean model: application to coastal ocean and estuaries. J. Atmos. Ocean. Technol. 20 (1), 159–186.
Chowdhury, Uttam K., Biswas, Bhajan K., Chowdhury, Tarit Roy, Samanta, Gautam, Mandal, Badal K., Basu, Gautam C., Chanda, Chitta R., Lodh, Dilip, Saha, Khitish C., Mukherjee, Subhas K., et al., 2000. Groundwater arsenic contamination in Bangladesh and West Bengal, India. Environ. Health Perspect. 108 (5), 393.
Church, J.A., Clark, P.U., Cazenave, A., Gregory, J.M., Jevrejeva, S., Levermann, A., Merrifield, M.A., Milne, G.A., Nerem, R.S., Nunn, P.D., Payne, A.J., Pfeffer, W.T., Stammer, D., Unnikrishnan, A.S., 2013. Climate Change 2013: the Physical Science Basis. Contribution of Working Group I to the Fifth Assessment Report of the Intergovernmental Panel on Climate Change. Cambridge University Press.
Clarke, D., Williams, S., Jahiruddin, M., Parks, K., Salehin, M., 2015. Projections of on-farm salinity in coastal Bangladesh. Environ. Sci.: Process. Impact 17, 1127–1136.
Clarke, Derek, Lázár, Attila N., Saleh, Abul Fazal M., Jahiruddin, Mohammad, 2018. Prospects for agriculture under climate change and soil salinisation. In: Ecosystem Services for Well-Being in Deltas. Palgrave Macmillan, Cham, pp. 447–467.
CSIRO, WARPO, BWDB, IWM, BIDS, CEGIS, 2014. Bangladesh Integrated Water Resource Assessment: Final Report Excerpted from Chapter 7 of Surface Water Assessment of Bangladesh and Impact of Climate Change. Institute of Water Modelling, Bangladesh and Commonwealth Scientific and Industrial Research, Australia.
Dai, Zhijun, Chu, Ao, Stive, Marcel, Zhang, Xiaoling, Yan, Hong, 2011. Unusual salinity conditions in the yangtze estuary in 2006: impacts of an extreme drought or of the three gorges dam? Ambio 40 (5), 496–505.
Dasgupta, Susmita, Kamal, Farhana Akhter, Khan, Zahirul Huque, Choudhury, Sharifuzzaman, Nishat, Ainun, 2014. River Salinity and Climate Change: Evidence from Coastal Bangladesh, vol. 6817. World Bank Policy Research Working Paper.
De Dominicis, Michela, Wolf, Judith, Jevrejeva, Svetlana, Zheng, Peng, Hu, Zhan, 2020. Future interactions between sea level rise, tides, and storm surges in the world's largest urban area. Geophys. Res. Lett. 47 (4) e2020GL087002.
Eslami, Sepehr, Hoekstra, Piet, Trung, Nam Nguyen, Ahmed Kantoush, Sameh, Van Binh, Doan, Tran Quang, Tho, van der Vegt, Maarten, et al., 2019. Tidal amplification and salt intrusion in the mekong delta driven by anthropogenic sediment starvation. Sci. Rep. 9 (1), 1–10.
FAO, 2016. Ganges-Brahmaputra-Meghna Basin.
Gallo, Marcos Nicolás, Vinzon, Susana Beatriz, 2005. Generation of overtides and compound tides in amazon estuary. Ocean Dynam. 55 (5–6), 441–448.
Galloway, William E., 1975. Process Framework for Describing the Morphologic and Stratigraphic Evolution of Deltaic Depositional Systems.
Gong, Zheng, Zhang, Chang-kuan, Wan, Li-ming, Zuo, Jun-cheng, 2012. Tidal level response to sea-level rise in the yangtze estuary. China Ocean Eng. 26 (1), 109–122.
Han, Weiqing, Meehl, Gerald A., Rajagopalan, Balaji, Fasullo, John T., Hu, Aixue, Lin, Jialin, Large, William G., Wang, Jih-wang, Quan, Xiao-Wei, Trenary, Laurie L., et al., 2010. Patterns of Indian Ocean sea-level change in a warming climate. Nat. Geosci. 3 (8), 546.
Haque, A., Sumaiya, Rahman, M., 2016. Flow distribution and sediment transport mechanism in the estuarine systems of ganges-brahmaputra-meghna delta. Int. J. Environ. Sustain Dev. 7 (22).
Haque, S.A., 2006. Salinity problems and crop production in coastal regions of Bangladesh. Pakistan J. Bot. 38 (5), 1359–1365.
Higgins, Stephanie A., Overeem, Irina, Rogers, Kimberly G., Kalina, Evan A., Chadwick, Oliver, Passalacqua, Paola, 2018. River linking in India: downstream impacts on water discharge and suspended sediment transport to deltas. Elementa: Sci. Anthropocene 6.
Hoitink, A.J.F., Jay, David A., 2016. Tidal river dynamics: implications for deltas. Rev. Geophys. 54 (1), 240–272.
Hong, Bo, Liu, Zhonghui, Shen, Jian, Wu, Hui, Gong, Wenping, Xu, Hongzhou, Wang, Dongxiao, 2020. Potential physical impacts of sea-level rise on the pearl river estuary, China. J. Mar. Syst. 201, 103245.
Horrevoets, A.C., Savenije, H.H.G., Schuurman, J.N., Graas, S., 2004. The influence of river discharge on tidal damping in alluvial estuaries. J. Hydrol. 294 (4), 213–228.
Howden, Stephan D., Murtugudde, Raghu, 2001. Effects of river inputs into the bay of bengal. J. Geophys. Res.: Oceans 106 (C9), 19825–19843.
Huq, SM Imamul, Shoaib, Jalaluddin Md, et al., 2013. The Soils of Bangladesh. Springer.
Islam, Mohammad Rezwanul, Yamaguchi, Yasushi, Ogawa, Katsuro, 2001. Suspended sediment in the ganges and brahmaputra rivers in Bangladesh: observation from TM and AVHRR data. Hydrol. Process. 15 (3), 493–509.
Jackson, Luke P., Jevrejeva, Svetlana, 2016. A probabilistic approach to 21st century regional sea-level projections using RCP and high-end scenarios. Global Planet. Change 146, 179–189.
Jahan, M., Chowdhury, M.M.A., Shampa, Rahman, M.M., Hossain, M.A., 2015. Spatial variation of sediment and some nutrient elements in GBM delta estuaries: a preliminary assessment. In: International Conference on Recent Innovation in Civil Engineering for Sustainable Development(IICSD-2015), vol. 6.
Jevrejeva, Svetlana, Jackson, Luke P., Riva, Riccardo EM., Grinsted, Aslak, Moore, John C., 2016. Coastal sea level rise with warming above 2 C. Proc. Natl. Acad. Sci. Unit. States Am. 113 (47), 13342–13347.
Johnson, F. Amoako, Hutton, C.W., Hornby, D., Lázár, A.N., 2016a. Is shrimp farming a successful adaptation to salinity intrusion? a geospatial associative analysis of poverty in the populous Ganges–Brahmaputra–Meghna Delta of Bangladesh. Sustain. Sci. 11 (3), 423–439.
Johnson, Fiifi Amoako, Hutton, Craig W., 2018. A geospatial analysis of the social, economic and environmental dimensions and drivers of poverty in South-West Coastal Bangladesh. In: Ecosystem Services for Well-Being in Deltas. Springer, pp. 383–403.
Johnson, Fiifi Amoako, Hutton, Craig W., Duncan, Hornby, Lázár, Attila N., Mukhopadhyay, Anirban, 2016b. Is shrimp farming a successful adaptation to salinity intrusion? a geospatial associative analysis of poverty in the populous Ganges–Brahmaputra–Meghna Delta of Bangladesh. Sustain. Sci. 11 (3), 423–439.
Kay, S., Caesar, J., Wolf, J., Bricheno, L., Nicholls, R.J., Saiful Islam, A.K.M., Haque, A., Pardaens, A., Lowe, J.A., 2015. Modelling the increased frequency of extreme sea levels in the Ganges-Brahmaputra-Meghna delta due to sea level rise and other effects of climate change. Environ. Sci.: Process. Impact 17, 1311–1322. https://doi.org/10.1039/C4EM00683F.
Khan, Aneire Ehmar, Ireson, Andrew, Kovats, Sari, Kumar Mojumder, Sontosh, Khusru, Amirul, Rahman, Atiq, Vineis, Paolo, 2011. Drinking water salinity and maternal health in coastal Bangladesh: implications of climate change. Environ. Health Perspect. 119 (9), 1328.
Khanom, Sayma, Salehin, Mashfiqus, 2012. Salinity constraints to different water uses in coastal area of Bangladesh: a case study. Bangladesh J. Sci. Res. 25 (1), 33–41.
Kundzewicz, Zbigniew W., 2008. Climate change impacts on the hydrological cycle. Ecohydrol. Hydrobiol. 8 (2–4), 195–203.
Lázár, Attila N., Clarke, Derek, Adams, Helen, Akanda, Abdur Razzaque, Szabo, Sylvia, Nicholls, Robert J., Matthews, Zoe, Begum, Dilruba, Saleh, Abul Fazal M., Abedin, Md Anwarul, et al., 2015. Agricultural livelihoods in coastal Bangladesh under climate and environmental change–a model framework. Environ. Sci.: Proces. Impact 17 (6), 1018–1031.
Leonardi, Nicoletta, Alexander, S Kolker, Fagherazzi, Sergio, 2015. Interplay between river discharge and tides in a delta distributary. Adv. Water Resour. 80, 69–78.
Li, Li, Wang, Xiao Hua, Williams, David, Sidhu, Harvinder, Song, Dehai, 2012. Numerical study of the effects of mangrove areas and tidal flats on tides: a case study of Darwin harbour, Australia. J. Geophys. Res.: Oceans 117 (C6), 1978–2012.
Liu, Bingjun, Peng, Sihan, Liao, Yeying, Long, Weili, 2018. The causes and impacts of water resources crises in the pearl river delta. J. Clean. Prod. 177, 413–425.
Matte, Pascal, Secretan, Yves, Morin, Jean, 2014. Temporal and spatial variability of tidal-fluvial dynamics in the st. lawrence fluvial estuary: an application of nonstationary tidal harmonic analysis. J. Geophys. Res.: Oceans 119 (9), 5724–5744.
Milliman, John D., Meade, Robert H., 1983. World-wide delivery of river sediment to the oceans. J. Geol. 1–21.
Murty, T.S., Henry, R.F., 1983. Tides in the bay of bengal. J. Geophys. Res.: Oceans 88 (C10), 6069–6076, 1978–2012.
Nahian, Mahin Al, Ahmed, Ali, Lázár, Attila N., Hutton, Craig W., Salehin, Mashfiqus, Streatfield, Peter Kim, 2018. Drinking Water Salinity Associated Health Crisis in Coastal bangladesh. Elementa: Science of the Anthropocene.

Nerem, Robert Steven, Beckley, Brian D., Fasullo, John T., Hamlington, Benjamin D., 2018. Dallas Masters, and Gary T Mitchum. Climate-change–driven accelerated sea-level rise detected in the altimeter era. Proc. Natl. Acad. Sci. Unit. States Am. 115 (9), 2022–2025.
Nhan, Nguyen Huu, 2016. Tidal regime deformation by sea level rise along the coast of the mekong delta. Estuar. Coast. Shelf Sci. 183, 382–391.
Nicholls, R.J., Hutton, C.W., Lázár, A.N., Allan, Andrew, Adger, W.N., Adams, Helen, Wolf, Judith, Rahman, Munsur, Salehin, Mashfiqus, 2016. Integrated assessment of social and environmental sustainability dynamics in the Ganges-Brahmaputra-Meghna delta, Bangladesh. Estuar. Coast. Shelf Sci. 183, 370–381.
Nicholls, Robert J., Mimura, Nobuo, 1998. Regional issues raised by sea-level rise and their policy implications. Clim. Res. 11 (1), 5–18.
Nienhuis, Jaap H., Ashton, Andrew D., Giosan, Liviu, 2015. What makes a delta wave-dominated? Geology 43 (6), 511–514.
Nienhuis, Jaap H., Hoitink, A.J.F., Törnqvist, Torbjörn E., 2018. Future change to tide-influenced deltas. Geophys. Res. Lett. 45 (8), 3499–3507.
Nienhuis, J.H., Ashton, A.D., Edmonds, D.A., Hoitink, A.J.F., Kettner, A.J., Rowland, J. C., Törnqvist, T.E., 2020. Global-scale human impact on delta morphology has led to net land area gain. Nature 577 (7791), 514–518.
Nishat, Bushra, Rahman, SM Mahbubur, 2009. Water resources modeling of the ganges-brahmaputra-meghna river basins using satellite remote sensing data 1. JAWRA J. Am. Water Res. Assoc. 45 (6), 1313–1327.
Pawlowicz, Rich, Beardsley, Bob, Lentz, Steve, 2002. Classical tidal harmonic analysis including error estimates in MATLAB using T_TIDE. Comput. Geosci. 28 (8), 929–937.
Payo, Andres, Mukhopadhyay, Anirban, Hazra, Sugata, Ghosh, Tuhin, Ghosh, Subhajit, Brown, Sally, Nicholls, Robert J., Bricheno, Lucy, Wolf, Judith, Kay, Susan, Lázár, Attila N., Haque, Anisul, 2016. Projected changes in area of the Sundarban mangrove forest in Bangladesh due to SLR by 2100. Climatic Change 139 (2), 279–291. https://doi.org/10.1007/s10584-016-1769-z. ISSN 1573-1480.
Payo, Andrés, Lázár, Attila N., Clarke, Derek, Nicholls, Robert J., Bricheno, Lucy, Mashfiqus, Salehin, Haque, Anisul, 2017. Modelling daily soil salinity dynamics in response to agricultural and environmental changes in coastal Bangladesh. Earth's Future 279–291.
Pethick, John, Orford, Julian D., 2013. Rapid rise in effective sea-level in southwest Bangladesh: its causes and contemporary rates. Global Planet. Change 111, 237–245.
Rahman, Afeefa, Yunus, Anika, 2016. Hydrodynamic and morphological response to dredging: analysis on gorai river of Bangladesh. Int. J. Innov. Res. Sci. Eng. Technol. 15610–15618.
Rahman, Munsur, Haque, Anisul, Siddique, Muhammad Khalid Bin, Rezaie, Ali Mohammad, Hafez, Md, Ahmed, Robert J., Darby, Stephen, Wolf, Judith, Sarker, Maminul Haque, Alam, Shah, et al., 2013. A preliminary assessment of the impact of fluvio-tidal regime on ganges-brahmaputra-meghna delta and its impact on the ecosystem resources. In: International Conference on Climate Change Impact and Adaptation (I3CIA-2013).
Rao, R.R., Sivakumar, R., 2003. Seasonal variability of sea surface salinity and salt budget of the mixed layer of the north indian ocean. J. Geophys. Res.: Oceans 108 (C1), 9–1.
Roy, Binata, Haider, Muhammad Rezaul, Yunus, Anika, 2016. A study on hydrodynamic and morphological behavior of padma river using delft3d model. In: Proceedings of the 3rd International Conference on Civil Engineering for Sustainable Development, vols. 12–14.
Saha, Nibir, Mondal, M., Humphreys, E., Bhattacharya, Jayanta, Rashid, M., Paul, Priya Lal, Ritu, S., 2015. Triple Rice in a Year: Is it a Feasible Option for the Low Salinity Areas of the Coastal Zone of bangladesh? 05.
Salehin, Mashfiqus, Chowdhury, Shahad Mahabub, Clarke, Derek, Mondal, Shahjahan, Nowreen, Sara, Jahiruddin, Mohammad, Haque, Asadul, 2018. Mechanisms and drivers of soil salinity in coastal Bangladesh. In: Ecosystem Services for Well-Being in Deltas. Springer, pp. 333–347.
Sassi, M.G., Hoitink, A.J.F., 2013. River flow controls on tides and tide-mean water level profiles in a tidal freshwater river. J. Geophys. Res.: Oceans 118 (9), 4139–4151.
Shaha, Dinesh Chandra, Cho, Yang-Ki, 2016. Salt plug formation caused by decreased river discharge in a multi-channel estuary. Sci. Rep. 6, 27176.
Sherif, Mohsen M., Singh, Vijay P., 1999. Effect of climate change on sea water intrusion in coastal aquifers. Hydrol. Process. 13 (8), 1277–1287.
Sherin, V.R., Durand, Fabien, Papa, Fabrice, Islam, AKM Saiful, Gopalakrishna, V.V., Khaki, M., Suneel, V., 2020. Recent salinity intrusion in the bengal delta: observations and possible causes. Continent. Shelf Res. 1–10, 104142.
Sinha, M., 2004. Farakka barrage and its impact on the hydrology and fishery of hooghly estuary. In: The Ganges Water Diversion: Environmental Effects and Implications. Springer, pp. 103–124.
Sohel, Nazmul, Persson, Lars Åke, Rahman, Mahfuzar, Streatfield, Peter Kim, Yunus, Muhammad, Ekström, Eva-Charlotte, Vahter, Marie, 2009. Arsenic in drinking water and adult mortality: a population-based cohort study in rural Bangladesh. Epidemiology 824–830.
Syvitski, James PM., Kettner, Albert J., Overeem, Irina, Hutton, Eric WH., Hannon, Mark T., Robert Brakenridge, G., Day, John, Vörösmarty, Charles, Saito, Yoshiki, Giosan, Liviu, et al., 2009. Sinking deltas due to human activities. Nat. Geosci. 2 (10), 681–686.
Tian, Richard, 2019. Factors controlling saltwater intrusion across multi-time scales in estuaries, chester river, chesapeake bay. Estuar. Coast. Shelf Sci. 223, 61–73.
Vousdoukas, Michalis I., Mentaschi, Lorenzo, Voukouvalas, Evangelos, Verlaan, Martin, Jevrejeva, Svetlana, Jackson, Luke P., Feyen, Luc, 2018. Global probabilistic projections of extreme sea levels show intensification of coastal flood hazard. Nat. Commun. 9 (1), 2360.
Wade, A.J., Durand, P., Beaujouan, V., Wessel, W.W., Raat, K.J., Whitehead, P.G., Butterfield, D., Rankinen, K., Lepisto, A., 2002. A nitrogen model for European catchments: INCA, new model structure and equations. Hydrol. Earth Syst. Sci. 6, 559–582.
Werner, Adrian D., Simmons, Craig T., 2009. Impact of sea-level rise on sea water intrusion in coastal aquifers. Groundwater 47 (2), 197–204.
White, Elliott, Kaplan, David, 2017. Restore or retreat? saltwater intrusion and water management in coastal wetlands. Ecosys. Health Sustain. 3 (1), e01258.
Whitehead, P.G., Barbour, E., Futter, M.N., Sarkar, S., Rodda, H., Caesar, J., Butterfield, D., Jin, L., Sinha, R., Nicholls, R., et al., 2015a. Impacts of climate change and socio-economic scenarios on flow and water quality of the Ganges, Brahmaputra and Meghna (GBM) river systems: low flow and flood statistics. Environ. Sci. Proces. Impact 1057–1069.
Whitehead, P.G., Sarkar, S., Jin, L., Futter, M.N., Caesar, J., Barbour, E., Butterfield, D., Sinha, R., Nicholls, R., Hutton, C., et al., 2015b. Dynamic modeling of the Ganga river system: impacts of future climate and socio-economic change on flows and nitrogen fluxes in India and Bangladesh. Environ. Sci.: Proces. Impact 1082–1097.
Wilson, Carol, Goodbred, Steven, Small, Christopher, Gilligan, Jonathan, Sams, Sarah, Mallick, Bishawjit, Hale, Richard, Chadwick, Oliver, Renaud, Fabrice, 2017. Widespread infilling of tidal channels and navigable waterways in the human-modified tidal deltaplain of southwest Bangladesh. Elementa: Sci. Anthropocene 5.
Ye, Yong, Tam, Nora Fung-Yee, Lu, Chang-Yi, Wong, Yuk-Shan, 2005. Effects of salinity on germination, seedling growth and physiology of three salt-secreting mangrove species. Aquat. Bot. 83 (3), 193–205.
Yuan, Rui, Zhu, Jianrong, 2015. The effects of dredging on tidal range and saltwater intrusion in the pearl river estuary. J. Coast Res. 31 (6), 1357–1362.
Zhang, Aijun, Wei, Eugene, 2007. Delaware river and bay hydrodynamic simulations with fvcom. In: Estuarine and Coastal Modeling, pp. 18–37, 2008.
Zhang, Zhiming, Cui, Baoshan, Zhao, Hui, Fan, Xiaoyun, Zhang, Honggang, 2010. Discharge-salinity relationships in modaomen waterway, pearl river estuary. Procedia Environ. Sci. 2, 1235–1245.